Numerical Simulation Study of Drag and Downforce on the Rear Wing of F1 Cars

Zhidong Guo(✉)

North China University of Technology, No. 5 Jinyuanzhuang Road, Shijingshan District, Beijing, China
1317703@qq.com

Abstract. The design of the aerodynamic profile of a good F1 car is very important, among which the rear wing plays a key role, and the downforce and drag caused by it are two key parameters to determine the aerodynamic performance. The aerodynamic characteristics of the rear wing of a Formula 1 car at different speeds were simulated using hydrodynamic calculation methods and commercial simulation software to find the best rear wing layout after comparing the effects of different angles of attack and different wing shapes on the aerodynamic performance of the car. The results show that the best aerodynamic effect of the rear wing is achieved with the Drela AG03 wing type at an angle of attack of about 20° and a speed of 21 km/h.

Keywords: Tailpiece Of F1 Racing · Downward Pressure · Resistance · Attack Angle · Wing Type

1 Introduction

In the process of designing and building a Formula One car, the speed of the car is undoubtedly the most important concern of the designer. Previous research has shown that the top speed of a race car is largely dependent not on the power of the engine, but on the grip of the car. [2] For the traditional racing car using tires, the driving force, steering force and braking force of the car need to be generated by the friction between the tires and the ground, and when the tangential force applied to the contact surface between the tires and the ground exceeds a certain limit, the tires will inevitably begin to slip and fail, and the car will be difficult to control, or even out of control. Without increasing the weight of the car, the aerodynamic shape of the rear wing to provide downforce and thus increase grip is the best solution today. [5] According to statistics, 20% of a car's grip is provided by its own weight and 80% is generated by the downforce provided by the rear wing. [6] Therefore, aerodynamics is one of the key technical issues concerning the performance of F1 cars today. In the aerodynamic design of the rear wing, downforce and drag are two key parameters to measure. [7] Downforce directly reflects the ability of the rear wing to provide grip, while drag reflects the effect of the aerodynamic shape of the rear wing on the driving process of the car. Finding a balance between these two

K. Subramanian et al. (Eds.): CTMCD 2022, ACSR 99, pp. 632–645, 2023.
https://doi.org/10.2991/978-94-6463-046-6_74

key parameters is the most important part of designing and manufacturing a good race car.

In this paper, we will use fluid simulation software to perform finite element analysis for different speeds, different angles of attack, and different airfoil shapes, and select the best tailplane start-up layout to meet the design requirements based on the results of the simulation data.

2 Computational Models

2.1 Racing Tail Aerodynamics

In order to get faster, a racing car must have enough grip, so it must increase the dead weight of the car, but the increased weight of the car will in turn affect the increase in speed. In order to solve such a deadly cycle, the American Chapparal first proposed the concept of negative lift wings. [1].

Racing car in the process of driving will be subject to longitudinal, lateral and vertical on the three directions of air resistance, by installing a racing rear wing can offset part of the air resistance in the process of driving, and generate a fourth force, that is, the downforce on the car, so that the car can be close to the road, thereby enhancing the stability of high-speed driving process. [3].

According to the Kuta-Jukovsky lift theorem, when an annulus is superimposed on the cylindrical winding flow of a straight homogeneous flow with uniform symmetry, it will generate a force that reverses the direction of 90° rotation of the annulus, and the magnitude of the force is related to the strength of the annulus. [4] When the tail of the racing car is in the straight uniform flow with velocity v, there exists a counterclockwise annulus with strength τ at the tail of the racing car. Assuming the velocity change brought about by the annulus in the flow superposition is Δv, the actual flow SU on the upper surface of the airfoil is v-Δv, while the flow velocity on the lower surface is v + Δv, at which time the flow velocity on the lower surface is greater than that on the upper surface. According to Bernoulli equation there are:

$$P + \frac{1}{2}\rho v^2 + \rho gh = C \tag{1}$$

where P is the pressure at a point in the fluid (Pa); v is the flow rate of the fluid at that point (m/s); p is the fluid density (kg/m3); g is the acceleration of gravity (m/s2); h is the height at that point (m); C is a constant.

When the speed of the upper surface of the airfoil is less than the speed of the lower surface, the pressure on the upper surface is greater than the lower surface, so the negative pressure is generated.

2.2 Control Equations and Turbulence Models

2.2.1 Control Equations

Since the controlling equation for racing is the Reynolds-averaged N-S equation for incompressible fluids.

Continuous equations.

$$\frac{\partial u_i}{\partial \mathrm{x}_i} = 0, \tag{2}$$

Momentum equation

$$\rho \frac{\partial u_i}{\partial_t} + \rho u_i \frac{\partial u_i}{\partial x_j} = \frac{\partial}{\partial x_j}\left[\mu_{eff}\left(\frac{\partial u_i}{\partial x_j} + \frac{\partial u_j}{\partial x_i}\right)\right] - \frac{\partial p'}{\partial x_i} \tag{3}$$

where, $\mathrm{u_i}$, $\mathrm{u_j}$ are velocity tensor; ρ is air density; p' is correction pressure; μ_{eff} is effective viscosity coefficient.

$$\mu_{eff} = \mu + \mu_t$$

2.2.2 Turbulence Model

After literature comparison and experimental comparison, it is considered that the ke model performs the best in running the simulation, so the ke model is chosen as the model used in the simulation。

The turbulent kinetic energy and turbulent energy dissipation equations for the k-ε model are,

\Turbulent energy equation κ

$$\frac{\partial(\rho k)}{\partial_t} + p\mathrm{u_i}\frac{\partial(\rho k u_i)}{\partial x_i} = \frac{\partial}{\partial x_j}\left[\left(\mu + \frac{\mu_t}{\sigma_k}\right)\frac{\partial k}{\partial x_j}\right] + \mathrm{G}_k - \mathrm{p} \in$$

Turbulent kinetic energy dissipation equation

$$\frac{\partial(p\varepsilon)}{\partial t} + \frac{\partial(p\varepsilon u_i)}{\partial x_i} = \frac{\partial}{\partial x_j}\left[\left(\mu + \frac{\mu_t}{\sigma_\varepsilon}\right)\frac{\partial \varepsilon}{\partial x_j}\right] + \frac{\varepsilon}{k}(\mathrm{C}_{\varepsilon 1}\mathrm{C}_k - \mathrm{C}_{\varepsilon 2}\rho\varepsilon)$$

where: μ is the laminar viscosity coefficient, turbulence constants C_μ=0.09, $C_{\varepsilon 1}$=1.44, $C_{\varepsilon 2}$=1.92, σ_ε=1.3 are empirical constants; μ_t is the turbulence viscosity coefficient and $\mu_t = \rho C_\mu \frac{k^2}{\varepsilon}$; $\mathrm{G_k}$ is the turbulent kinetic energy generated by the laminar velocity gradient, $G_k = \mu_t\left(\frac{\partial u_i}{\partial x_j} + \frac{\partial u_j}{\partial x_i}\right)\frac{\partial u_i}{\partial x_j}$

2.3 3D Modelling and Meshing

2.3.1 3D Modelling

The flow field of the tailplane was created using Solidworks using a right handed coordinate system with the X-axis pointing to the right of the tailplane, the Z-axis pointing to the front of the tailplane and the Y-axis pointing to the bottom of the tailplane with the origin being the geometric centre of the flow field.

The XYZ point coordinates of the airfoil are first entered into Solidworks, a sketch is generated, the airfoil solid is stretched out and scaled appropriately, then the flow

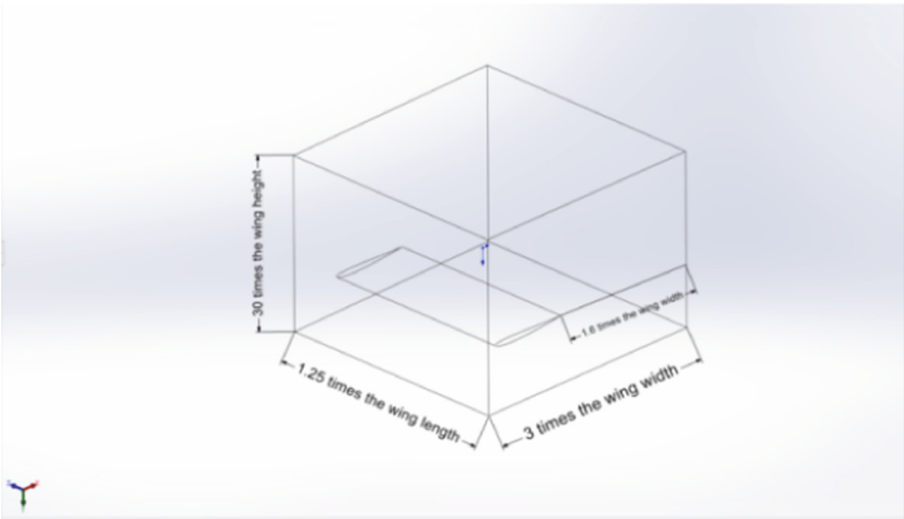

Fig. 1. Tail Flow Field

field solid is created and Boolean operations are performed with the tail entity. The flow field entity is a rectangular body with the geometric centre as the origin of the coordinate system, the length is approximately 1.25 times the wing length, the width is approximately 3 times the wing width, the height is approximately 30 times the wing height, the lower wing surface is approximately 8 times the wing height from the bottom surface, the front of the wing is 0.4 times the wing width and the back of the wing is 1.6 times the wing width, as shown in the figure below (Fig. 1).

As a variety of wing types were tested in this paper, the scaling varies slightly depending on the wing type, but the dimensions are basically the same.

2.3.2 Grid Division

Mesh delineation using Ansys Discovery aim software, with boundary layers defined as smooth transitions, a conversion ratio of 0.272, a maximum number of layers of 5, a growth rate of 1.2 and a cell shape of tetrahedron (Fig. 2).

2.3.3 Grid-Independent Solution Verification

In general, the higher the number of cells, the more accurate the solution will be, but too many cells will greatly increase the burden on the computer to solve, therefore, in order to obtain as accurate results as possible while saving computational resources, we carried out the verification of grid-independent solutions, each verification was performed twice, the number of cells between 300,000 ~ 630,000, the results of the solution for the maximum pressure, minimum pressure, lower pressure and resistance, the results are as follows (Table 1).

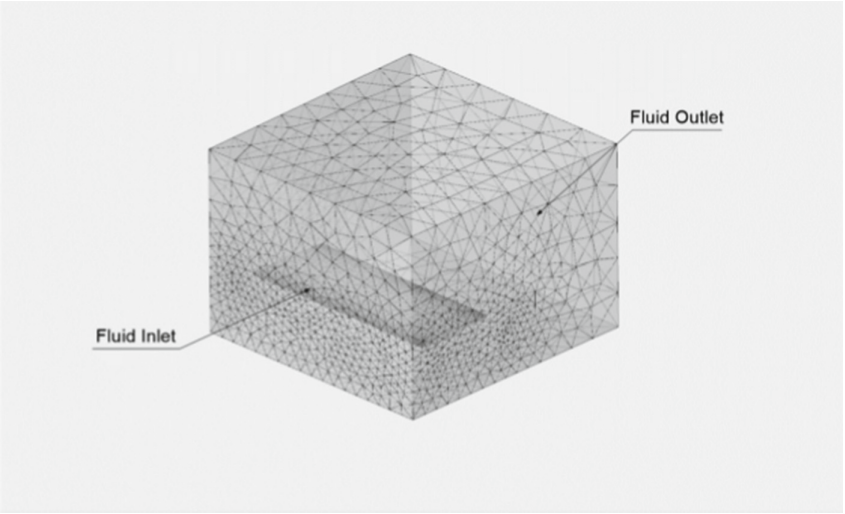

Fig. 2. Meshing of the tail flow field

Table 1. Effect of different number of cells on simulation results.

Number of simulations	Number of cells	Maximum pressure pa	Minimum pressure pa	Inlet velocity m/s	Down pressure N	Resistance N
1	$5.1x10^5$	2052.8	-856.13	60	454.79	51.485
2	$3x10^5$	1765.3	-856.96	60	467.85	53.328
1	$6.3x10^5$	2816.4	-1171.5	70	647.57	70.408
2	$3x10^5$	2401.5	-1168.3	70	638.3	70.873
1	$6.3x10^5$	3678.1	-1526	80	822.37	89.641
2	$3x10^5$	3519.4	-1677.1	80	825.87	90.423
1	$5.1x10^5$	4619.5	-1933.4	90	1017	108.12
2	$3x10^5$	4451.7	-2123.7	90	1046.9	112.42
1	$5.1x10^5$	5701.1	-2389.2	100	1257.2	131.24
2	$3x10^5$	4898.3	-2396.9	100	1308.7	136.91

Based on the validation results, it can be seen that the difference between the calculated values of the solutions is not too large when the number of cells is between 300,000 and 630,000.

A single main wing solution is proposed for this simulation study, aiming to reduce the total mass of the tailplane, reduce the tooling cost and increase the reliability of the simulation results.

3 Study of the Key Parameters of the Aerodynamic Performance of the Tailplane

3.1 Preceding Variable Settings

In order to determine the appropriate operating interval for the tail stabiliser, three sets of independent variables are set in this section: the speed at which the car is travelling, the angle of attack of the tailplane and the tailplane wing shape. In this series of simulations, the parameter range that allows the tail fin to operate optimally will be determined.

The simulation condition is steady-state flow, the fluid area material is ideal fluid air, the medium density is taken as the default value of air density: 1.18415kg/m^3, the viscosity is about 1.8x10^{-5}kg/(m.s).

3.2 With Wing Shape as the Independent Variable

Under the same driving speed and angle of attack, the different airfoil types will also have different effects on the performance of the rear wing in improving the grip. Airfoil, Drela AG08 airfoil, Drela AG09 airfoil, which are abbreviated as a,b,c,d,e in the table below.

The speed in this simulation is set to 64m/s and the angle of attack is 0° (Fig. 3).

As can be seen from the Ansys Discovery aim simulation post-processing and data, for a given speed and angle of attack, the different airfoil shapes have an effect on the downforce and drag that can be generated by a racing car. The table shows that the Drela AG03 (flat aft bottom) airfoil has the highest ratio of downforce to drag, 11.05, and therefore has the best aerodynamic performance.

3.3 With the Speed at Which the Car is Travelling as the Independent Variable

When the airfoil shape and angle of attack are certain, the change of the driving speed of the car will have an effect on the aerodynamic performance of the tail fin. Referring to the average speed of a real F1 car in a real race, this simulation set the car's travel speed as the independent variable and set 5 groups: 60m/s, 70m/s, 80m/s, 90m/s, 100m/s. The following table was made based on the data from the simulation.

The airfoil is set to Drela AG03 (flat aft bottom) airfoil and the angle of attack is 0° (Fig. 4).

As can be seen from the Ansys Discovery aim simulation post-processing and data, the higher the speed, the higher the maximum and minimum pressure on the airfoil, and the higher the drag and downforce caused by the tail fin, for a given airfoil shape and

angle of attack. On the other hand, the difference between the maximum and minimum pressure on the airfoil is smallest at a speed of 60m/s, and the rate of increase in drag is higher than the rate of increase in downforce as the car increases speed from 60m/s to 100m/s.

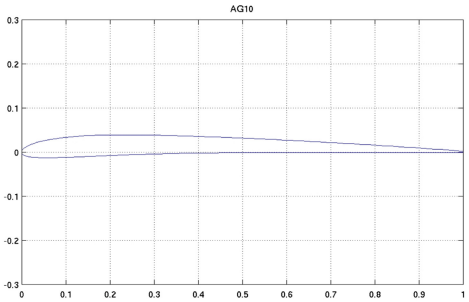

a) Drela AG10 airfoil

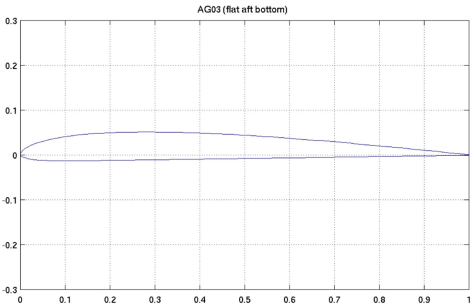

b)Drela AG03 (flat aft bottom) airfoil

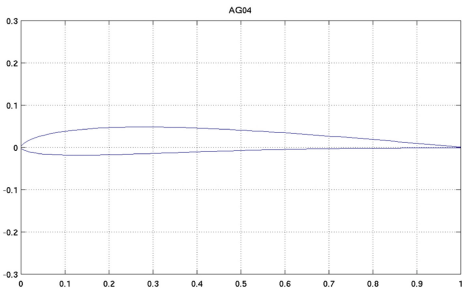

c)Drela AG04 airfoil

Fig. 3. Different airfoil shapes and their aerodynamic performance

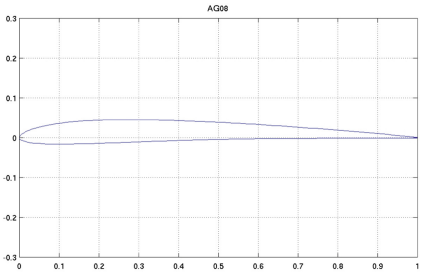

d) Drela AG08 airfoil

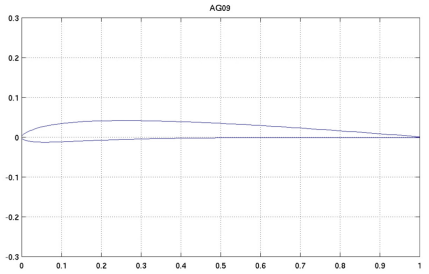

e) Drela AG09 airfoil

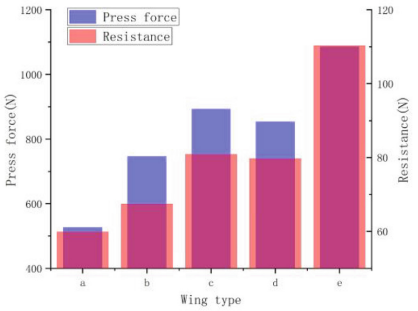

f) Downforce and drag variation characteristics of different airfoil types

Fig. 3. (*continued*)

3.4 With the Angle of Attack of the Tail as the Independent Variable

The angle of attack of the tailplane is also an important parameter affecting the aerodynamic performance of the tailplane. The angle of attack is the size of the angle between the airfoil and the oncoming airflow, an appropriate angle of attack can effectively improve the aerodynamic performance of the tailplane of the racing car, but too large an angle of attack will increase the air resistance and hinder the driving of the racing car. In this set of simulations, the angle of attack of the rear wing is used as the independent variable, and

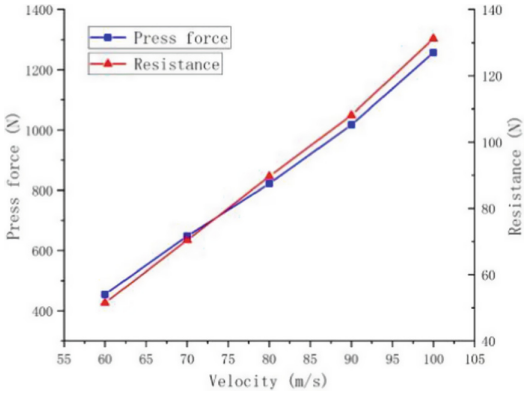

Fig. 4. Variation of downforce and resistance with velocity

five groups are set: 10°, 20°, 30°, 40° and 50°. Based on the data from the simulations, the following table was made.

In this simulation the airfoil is set to Drela AG03 (flat aft bottom) airfoil with a speed of 64m/s (Fig. 5).

Ansys Discovery aim simulation and data show that for a given wing shape and speed, the drag value increases at an average rate of 161.7% while the downforce increases slowly at an average rate of 27.7% when the angle of attack is greater than 45°.

3.5 With the Speed of the Car and the Angle of Attack of the Rear Wing as Independent Variables

As F1 cars do not travel at a constant speed, it is generally accepted that the driver needs to adjust the angle of attack of the rear wing at different driving speeds to obtain the highest grip and thus the best driving experience. This set of simulations will be set up with five sets of independent variables, one for the driving speed and one for the angle of attack of the rear wing. They are: driving speed: 60m/s, tail angle of attack: 10°, 20°, 30°, 40°, 50°, driving speed: 70m/s, tail angle of attack: 10°, 20°, 30°, 40°, 50°, driving speed: 80m/s, tail angle of attack: 10°, 20°, 30°, 40°, 50°, driving speed: 90m/s, tail angle of attack: 10°, 20°, 30°, 40°, 50°, travel speed: 100m/s, tail angle of attack: 10°, 20°, 30°, 40°, 50°, the following table was made based on the data from the simulation.

The airfoil is set to Drela AG03 (flat aft bottom) airfoil in this simulation (Fig. 6).

The Ansys Discovery aim simulation and data show that the angle of attack-xy pressure diagram is basically the same when changing the angle of attack of the rear wing at different speeds: at an angle of attack of 20°, the ratio of downforce to drag is the largest, so the driver only needs to control the angle of attack of the rear wing at about 20° to get the best driving experience during the F1 race.

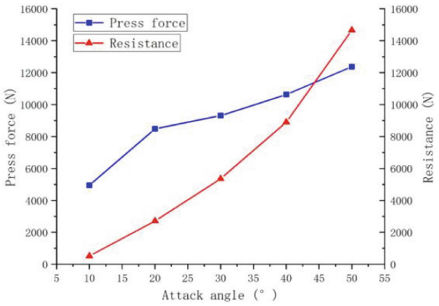

a)Variation of downforce and resistance with angle of attack

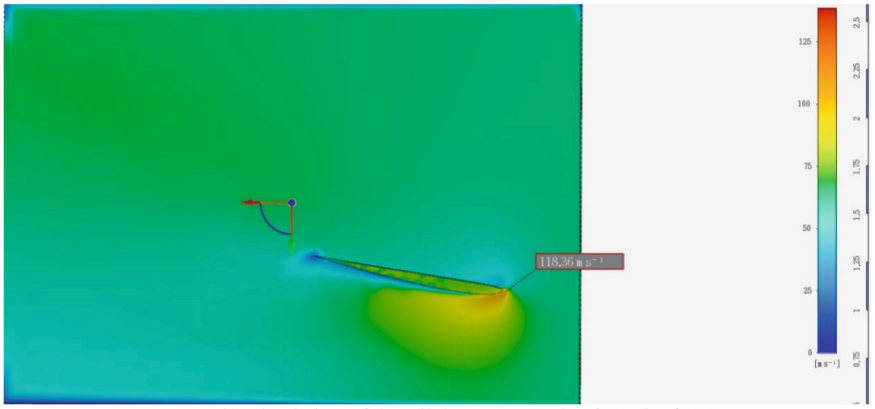

b) Cloud view of the tailplane at an angle of attack of 10°

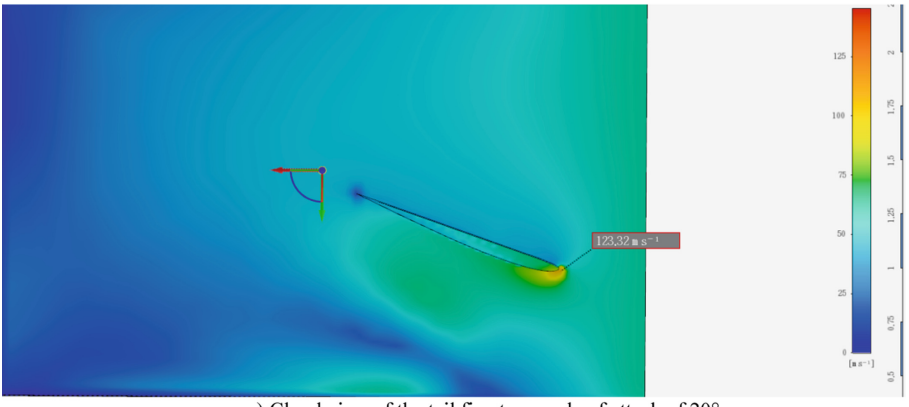

c) Cloud view of the tail fin at an angle of attack of 20°

Fig. 5. Pressure clouds at different angles of attack

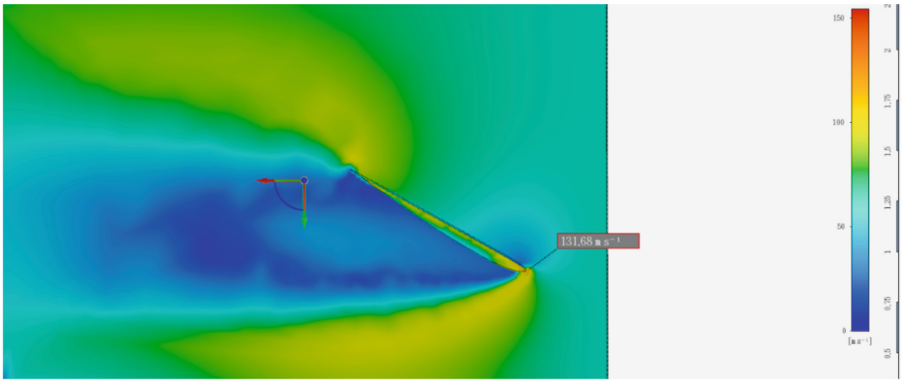

d) Cloud view of the tail fin at an angle of attack of 30°

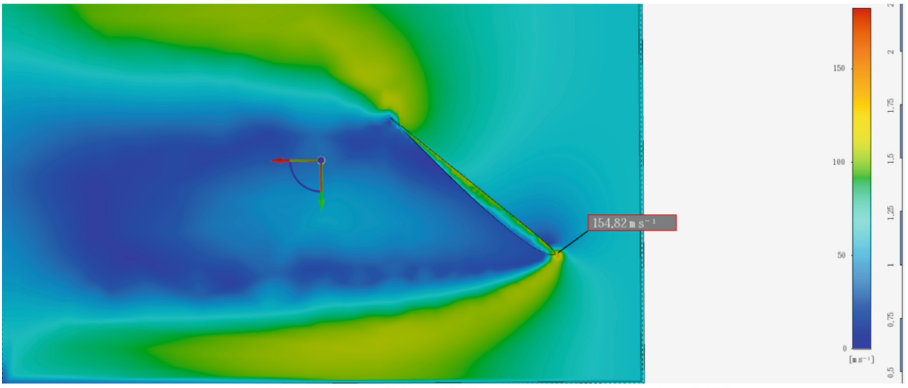

e) Cloud view of the tail fin at an angle of attack of 40°

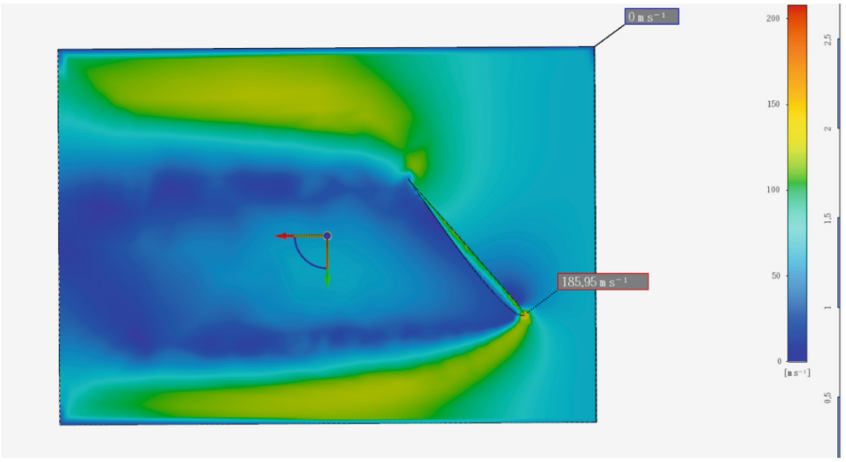

f) Cloud view of the tail fin at an angle of attack of 50°

Fig. 5. (*continued*)

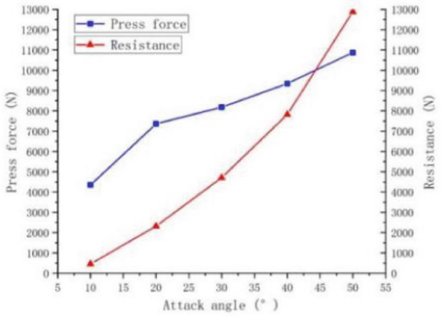

a) When velocity =60m/s ， variation of downforce and resistance with angle of attack

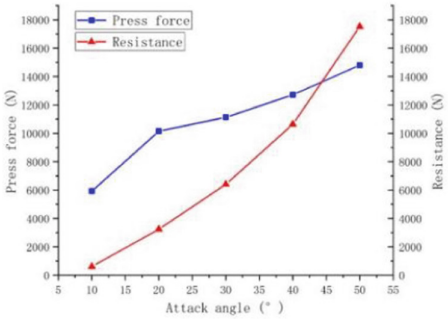

b) When velocity =70m/s ， variation of downforce and resistance with angle of attack

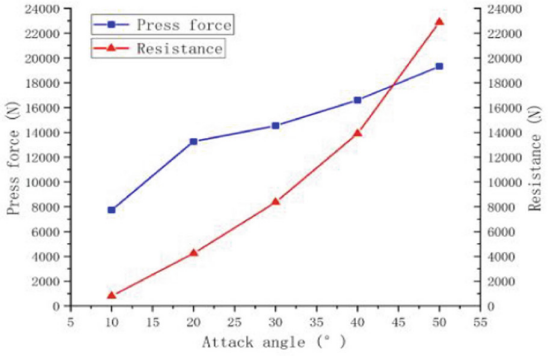

c) When velocity =80m/s ， variation of downforce and resistance with angle of attack

Fig. 6. Downforce and resistance curves at different speeds

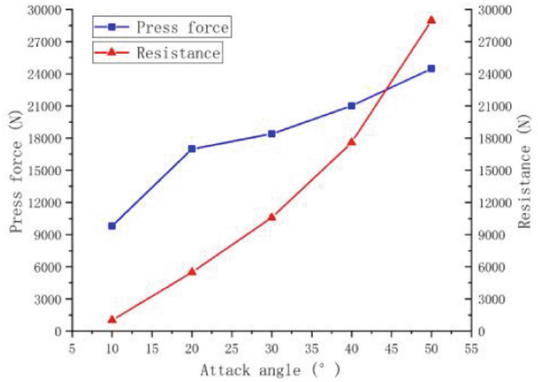

d) When velocity =90m/s，variation of downforce and resistance with angle of attack

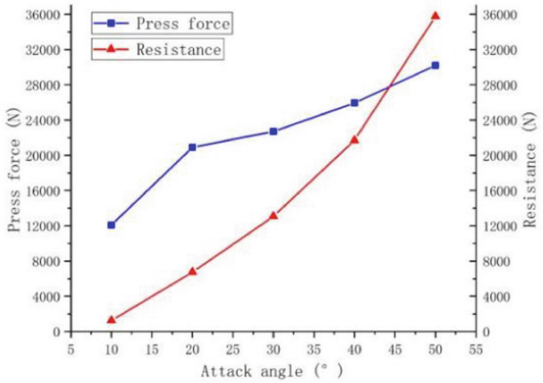

e) When velocity =100m/s，variation of downforce and resistance with angle of attack

Fig. 6. (*continued*)

4 Conclusion

In order to find the optimum operating parameters for the rear wing of a Formula 1 car, Solidworks was used for modelling and Ansys Discovery aim software for fluid simulation. The speed, angle of attack and wing shape of the rear wing were set as independent variables, and the downforce and drag were set as dependent variables.

(i) When comparing the downforce and drag for different airfoil types at the same speed and angle of attack, the ratio of downforce to drag was the highest with the Drela AG03 (flat aft bottom) airfoil type.

(ii) The faster the car travels, the greater the downforce and drag, but the drag tends to increase more than the downforce.

③The greater the angle of attack of the rear wing, the greater the drag, but the change in downforce is distributed in a zigzag pattern, peaking at 20°.

④The images of the angle-of-attack-xy pressure diagram obtained by changing the angle of attack at different driving speeds of the F1 car are basically the same, i.e. the ratio of downforce to drag is greatest when the angle of attack of the rear wing of the car is about 20°, and the car gets the best driving experience.

Therefore, it was verified that the optimum operating parameters for the tailfoil of a Formula 1 car during driving should be: Drela AG03 (flat aft bottom) airfoil, driving speed 60m/s and angle of attack around 20°.

References

1. Mao Xu, Wu Ning, Aerodynamic Performance Improvement of a New Type for Formula[J], Mechanical Science and Technology for Aerospace Engineering, 2014, 33(9): 1003-8728
2. Wang Da, Zhang Guoqing, Zhou Fuqiu, et al, Design and Performance Research on Active Aerodynamic Balance Device of Formula Student[C], Proceedings of the Annual Meeting of the Chinese Society of Automotive Engineering, 2021
3. Wang Jiapeng, Wang Yiping, Xia Yuchen, et al.. Optimization Design of Front Wing of FSAR Racing Car[C], Proceedings of the Annual Meeting of the Chinese Society of Automotive Engineering, 2021
4. Yan Zeyuan, Du Changqing, Hu Yifeng, et al, Study on aerodynamic performance of rear wing for Formula SAE racing cars based on finite element method[J], Journal of Chongqing University, 2019, 42(4): 1000-582x
5. Zhang Yufei, Li Chuanchang, Qiu Yiming, CFD Simulation Research and Analysis of Racing Car Intelligent Adjusting Rear Wing[C], Proceedings of the Annual Meeting of the Chinese Society of Automotive Engineering, 2021
6. Zhou Tao, Zeng Zhong, Optimal aerodynamic design for formula SAE car using curved wings[J], Journal of Chongqing University, 2017, 40(10): 1000-582x
7. Zhu Junlin, Yu Shichen, The Optimization of the Shape of FSAE Racing Car Spoiler[C], Proceedings of the Annual Meeting of the Chinese Society of Automotive Engineering, 2020